CONCEPTUAL DESIGN OF BOOSTER SYNCHROTRON FOR TPS

H. C. Chao*, J. W. Tsai, H. P. Chang, H. J. Tsai, P. J. Chou, G. H. Luo, and C. C. Kuo
NSRRC, Hsinchu 30076, Taiwan, R. O. C.

Abstract

Preliminary studies of booster for Taiwan Photon Source (TPS) include linear lattice, dynamic aperture, geometry allocation. The structure consists of modified FODO lattice with defocusing quadrupole fields built in bending magnets. The designed emittance is less than 10 nm-rad at 3 GeV. In this paper, the phenomena during the ramping from 150 MeV to 3.0 GeV, including the eddy current effect, the evolutions of beam emittance, energy spread, and bucket acceptance, will also be discussed. In addition, aperture request as well as closed orbit correction scheme are described.

INTRODUCTION

After long discussions, the TPS booster is designed to be sharing the same tunnel with the storage ring. One of the main reasons is the limited available space on the existing site. The TPS storage ring consists of 24 periods of DBA cells, with a 6-fold symmetry. It has six 12 m long straight sections and eighteen 7 m long standard straight sections. The circumference of the storage ring is 518.4 m. With the 500 MHz RF frequency, the storage ring harmonic number is 864. A reasonable tunnel space is needed to allow the installation of equipments and it is found at least around 20-m difference in circumference. The harmonic number of the concentric booster is chosen to be 828 with same RF frequency so that they have the common factor of 36. Hence the circumference of the booster is 496.8 m. The average space between beam centers of these two rings is around 3.44 m.

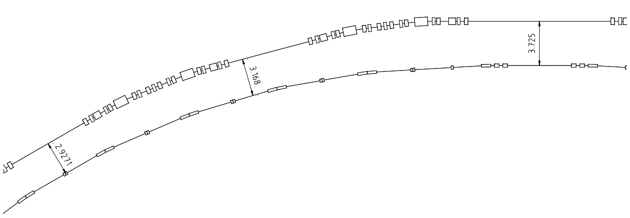

Figure 1: Layout of 1/12 of storage ring and booster ring

The geometry of the booster has six-fold symmetry to fit the shape of storage ring outside. There are six long straight sections which are non-dispersive and 5.37 m long each. Figure 1 shows the lattice of one-twelfth of the storage and booster ring. The minimal distance from beam center to beam center is around 2.92 m, wheras the maximal is around 3.73 m.

* hjjhao@nsrrc.org.tw

LATTICE

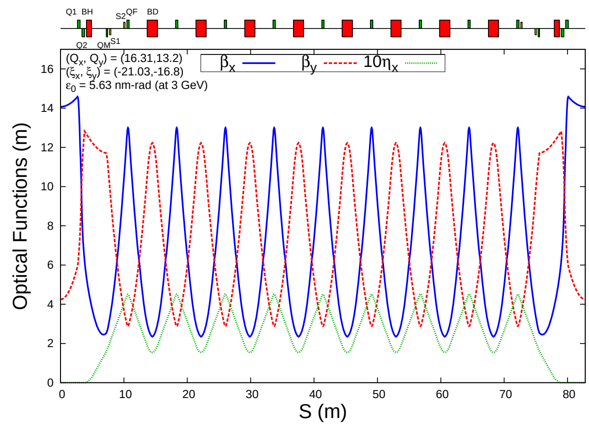

Figure 2: Optical functions of one superperiod

Table 1: Booster ring parameters

Circumference	496.8 m
Straight section length	5.37 m
Harmonic number	828
RF frequency	499.654 MHz
Betatron tune	16.313/13.197
Natural chromaticity	-21.0/-16.8
Damping partition	1.91/1.00/1.09
Energy spread at 3 GeV	0.09368 %
Natural emittance at 3 GeV	5.64 nm-rad
Damping time at 3 GeV	9.98/19.08/17.54 msec
Energy loss per turn at 3 GeV	521 KeV
Repetition rate	2 Hz

A number of different lattice structures were explored, and we chose a modified FODO lattice structure for the TPS booster design. There are 6 superperiods. Each superperiod consists of 8 cells of a combined function FODO lattice. The defocusing quadrupole and sextupole field components are part of the bending magnet (BD) pole geometry. The quadrupoles (QF) are separate and provide the focusing. They also include focusing sextupole field components. Each BD magnet is 1.6 m long with a bending angle of 6.667 degree. So the dipole field is 0.73 Tesla at 3 GeV and 363 Gauss at 150 MeV. The dispersion supressor at the end of each superperiod consists of one matching quadrupole (QM) and a separated function dipole, BH, with half the length and angle of the BD. Pairs of extra sextupoles (S1 and S2) are put in dispersion supressor section to correct the chromaticities during ramping. Outside BH there are two families of quadrupoles (Q1 and Q2) for matching the beta functions in straight sections. The optical functions are shown in figure

2 and the basic parameters of the booster are listed in table 1.

Tolerance to magnet errors is shown. 1 % of gradient error in every BD causes a ring tune shift of (-0.036, +0.162), and it can be corrected by Q1 and Q2. The dynamic aperture with and without multipole field errors are shown in figure 3. Particles are tracked for 1024 turns by the tracking code TRACY2 for both on and off-momentum.

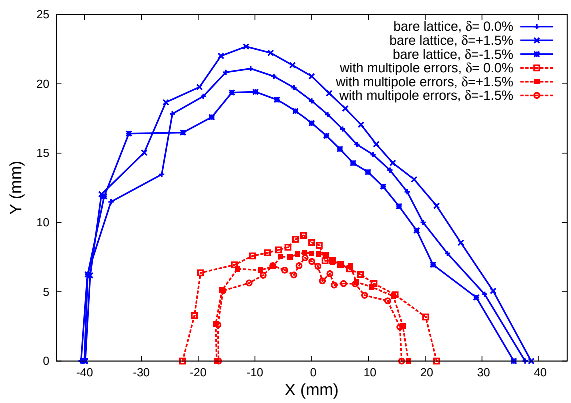

Figure 3: Dynamic aperture tracking

APERTURE REQUEST

Closed orbit distortions are due to dipole field and alignment errors. They are simulated under the following situations. The rms dipole field errors are 0.1 %. We assume the rms misalignments as δx = 0.15 mm, δy= 0.15 mm, and $\delta\theta$(roll) = 0.2 mrad for quadrupoles and δx = 0.20 mm, δy = 0.15 mm, and $\delta\theta$(roll) = 0.2 mrad for bending magnets. Errors larger than three times the rms values are truncated.

The SVD method is used to correct the orbit distortion. There are in total 66 horizontal correctors, 60 vertical correctors and 66 BPMs used in the orbit correction scheme. The average orbit distortion before correction are 3.27 mm in horizontal direction and 2.19 mm in vertical direction. After correction, the average orbit distortion can be less than 0.3 mm.

The beam aperture requirement is estimated from the beam size, COD, and off energy deviation using the following relations

- Aperture X = $\pm[a\sigma_x + bCOD_x(\text{rms}) + \eta_x\delta(\delta = 1\%)]$
- Aperture Y = $\pm[a\sigma_y + bCOD_y(\text{rms})]$

where σ_x and σ_y are the maximum horizontal and vertical beam size in the booster at injection. Here we use the beam parameters from the 150 MeV linac specifications. Both horizontal and vertical beam emittance are 167 nm-rad and the energy spread of the beam is 0.4 %. CODx and CODy are the root mean squared orbit distortion and $\eta_x\delta$ is for the orbit of 1 % off energy particles.

Before and after orbit corrections, different sets of the constants a and b are chosen accordingly. Table 2 shows the beam aperture requirement estimation. The required chamber size is an elliptical chamber with inner radii of 35 mm and 20 mm. The horizontal maximum beam stay clear occurs at QF, while the vertical takes place at BD.

Table 2: beam aperture requirement

	beam size (mm)	COD (mm)	$\eta_x\delta$ (mm)	BSC (mm)
before orbit correction horizontal beam stay clear	4.66 (a=2)	7.12 (b=2.5)	4.52 (δ=1%)	±16.30
before orbit correction vertical beam stay clear	2.92 (a=2)	7.20 (b=2.5)		±10.12
after orbit correction horizontal beam stay clear	6.99 (a=3)	2.88 (b=1)	4.52 (δ=1%)	±14.36
after orbit correction vertical beam stay clear	4.38 (a=3)	5.76 (b=2)		±10.14

RAMPING BEHAVIOR

The evolution of beam emittance obeys the following equation where τ_∞ represents the damping time at 3 GeV, γ the Lorentz factor, and f the revolution frequency.

$$\frac{\varepsilon_N(t)}{f dt} = -\left[\frac{1}{\gamma(t)}\frac{d\gamma(t)}{f dt} + \frac{2}{f\tau_\infty}\left(\frac{\gamma(t)}{\gamma_f}\right)^3\right]\varepsilon_N(t) + \frac{2}{f\tau_\infty}\left(\frac{\gamma(t)}{\gamma_f}\right)^5$$

The beam emittance normalized to the equilibrium state at the final ramping energy γ_f is $\varepsilon_N = \varepsilon/\varepsilon_\infty$. Figure 4 shows the evolution of the emittance during ramping at a repetition rate of 2 Hz. Here we assume for the vertical emittance at extraction at coupling ratio of 10 %.

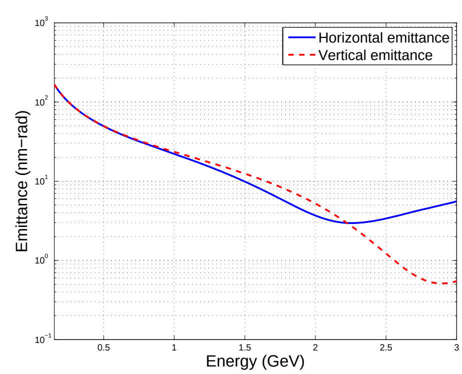

Figure 4: Emittance evolution curve

The evolution of beam energy spread obeys the following equation.

$$\frac{\sigma_N(t)}{f dt} = -\left[\frac{1}{4\gamma(t)}\frac{d\gamma(t)}{f dt} - \frac{1}{f\tau_\infty}\left(\frac{\gamma(t)}{\gamma_f}\right)^3\right]\sigma_N(t) + \frac{1}{f\tau_\infty}\left(\frac{\gamma(t)}{\gamma_f}\right)^7\frac{1}{\sigma_N}$$

Again, $\sigma_N = \sigma/\sigma_\infty$ represents the beam energy spread normalized to the equilibrium energy spread (σ_∞) at the final ramping energy γ_f. The energy is increased in a sinusoidal way from 150 MeV to 3 GeV while the cavity voltage is linearly ramped from 0.2 MV to 0.9 MV during half a ramping cycle. The ramping curves are shown in figure 5. The evolution of beam energy spread and acceptance during ramping are shown in figure 6. The large swing of energy acceptance allows only for 3 successive bunches to be injected from Linac at 150 MeV.

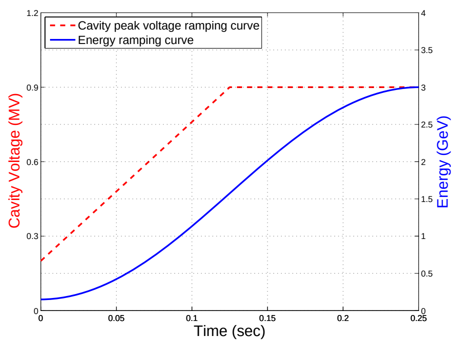

Figure 5: Ramping curve with the repetition rate 2 Hz

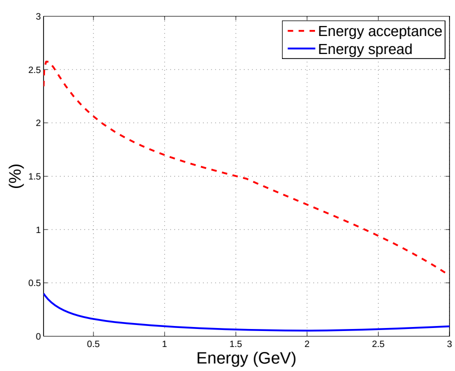

Figure 6: Energy acceptance and energy spread evolution

EDDY CURRENT EFFECT

For the sinusoidal ramping, the magnetic field as a function of time can be written as

$$B_y(t) = \frac{B_0}{2}(\alpha - \cos(\omega t)),$$

where $B_0 = B_{max} - B_{min}$, $\alpha = \frac{B_{max}+B_{min}}{B_{max}-B_{min}}$ and $\omega = 2\pi f$ is the repetition rate. The sextupole field induced by the eddy currents in the elliptic vacuum chamber in the bending magnets is given by

$$\Delta K_2 = \frac{1}{B\rho}\frac{\partial^2 B_y}{\partial x^2} = \mu_0 \sigma \frac{d}{h\rho}\frac{\dot{B}}{B} F\left(\frac{b}{a}\right),$$

where the form factor F is defined as

$$F\left(\frac{b}{a}\right) = \int_0^{\pi/2} \sin\phi \sqrt{\cos^2\phi + \left(\frac{b}{a}\right)^2 \sin^2\phi d\phi}$$
$$= \frac{1}{2}\left[1 + \frac{b^2 \sinh^{-1}(\sqrt{a^2-b^2}/b)}{a\sqrt{a^2-b^2}}\right],$$

$\mu_0 = 4\pi \times 10^{-7}$ is the vacuum permeability, $\sigma = 1.11 \times 10^6 [\Omega^{-1} m^{-1}]$ the conductivity of stainless steel, a/b is the vacuum chamber half-width/height, h the half-height of the dipole gap, ρ the bending radius, and d the chamber thickness. For the booster vacuum chamber, $F \approx 0.73$, and the variation of the chromaticities due to eddy currents during ramping are shown in figure 7. Extra sets of sextupoles are used to keep the chromaticities close to zero. The largest chromaticity changes take place at 35 msec, which requires a correction strength of S1[K_2] = 0.007 and S2[K_2] = -0.036(1/m^3) to keep the chromaticities close to (+1, +1).

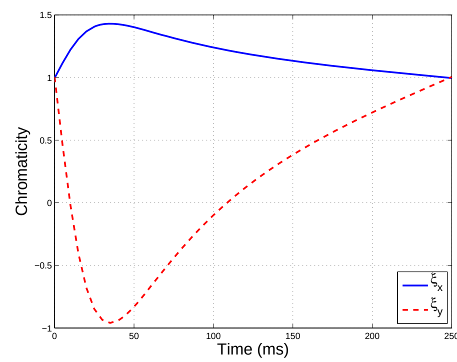

Figure 7: Eddy current effect

ACKNOWLEDGEMENTS

The authors would like to thank the colleagues of the beam dynamics group of NSRRC for their assistance.

REFERENCES

[1] M. Sands, “The Physics of Electron Storage Rings – An Introduction”.

[2] K. K. Lin and K. C. Cheng, “Ramping Behavior of Booster Synchrotron”, SRRC/IJ/IM/88-01.

[3] G. Hemmie and J. Rossbach, “Eddy Current Effects in the DESY II Dipole Vacuum Chamber”, DESY M-84-05 April 1984.